Direct Observation of Surface Ethyl to Ethane Interconversion upon C_2H_4 Hydrogenation over Pt/Al_2O_3 Catalyst by Time-Resolved FT-IR Spectroscopy

Walter Wasylenko and Heinz Frei*

Physical Biosciences Division, Lawrence Berkeley National Laboratory, University of California, Berkeley, California 94720

Received: July 8, 2005

Time-resolved FT-IR spectra of ethylene hydrogenation over alumina-supported Pt catalyst were recorded at 25 ms resolution in the temperature range of 323−473 K using various H_2 concentrations (1 atm total gas pressure). Surface ethyl species (2870 and 1200 cm^{-1}) were detected at all temperatures along with the gas-phase ethane product (2954 and 2893 cm^{-1}). The CH_3CH_2Pt growth was instantaneous on the time scale of 25 ms under all experimental conditions. At 323 K, the decay time of surface ethyl (122 ± 10 ms) coincides with the rise time of ethane (144 ± 14 ms). This establishes direct kinetic evidence for surface ethyl as the relevant reaction intermediate. Such a direct link between the temporal behavior of an unstable surface intermediate and the final product in a heterogeneous catalytic system has not been demonstrated before. A fraction (25%) of the asymptotic ethane growth at 323 K is prompt, indicating that there are surface ethyl species that react much faster than the majority of the CH_3CH_2Pt intermediates. The dispersive kinetics is attributed to the varying strength of interaction of the ethyl species with the Pt surface caused by heterogeneity of the surface environment. At 473 K, the majority of ethyl intermediates are hydrogenated prior to the recording of the first time slice (24 ms), and a correspondingly large prompt growth of ethane is observed. The yield and kinetics of the surface ethylidyne are in agreement with the known spectator nature of this species.

1. Introduction

Efforts to understand the detailed mechanism of heterogeneous catalytic hydrogenation of ethylene over noble metal catalysts continues to be of intense interest despite the large number of studies on this subject by many groups.[1,2] Hydrogenation of alkenes is of major industrial importance,[3] and the prototype C_2H_4 system has long served as a main focus for advancing the knowledge of this reaction type. In particular, vibrational spectroscopic studies of the reaction over single-crystal Pt surfaces or finely dispersed Pt particles on silica or alumina under steady-state conditions[1,2] led to the acceptance of a stepwise hydrogenation mechanism originally proposed by Horiuti and Polanyi.[4] In this mechanism, surface-adsorbed ethylene is hydrogenated to ethyl and subsequently converted to ethane.

$$C_2H_4 + Pt{-}H \rightarrow CH_3CH_2Pt \quad (1)$$

$$CH_3CH_2Pt + Pt{-}H \rightarrow C_2H_6 + Pt \quad (2)$$

Adsorbed ethylene is known to exist in a weakly π-bonded or more strongly di-σ-bonded form based on reflection−absorption infrared and HREELS studies on Pt(111) surfaces[5−9] and transmission IR spectroscopy of supported metal particle catalysts.[10,11] Various experimental studies have provided convincing evidence that the hydrogenation step (1) involves π-C_2H_4 species.[12−15] Using sum frequency generation spectroscopy (SFG) for monitoring the CH stretching region, Somorjai and co-workers have identified absorption bands of π-bonded and di-σ-ethylene over Pt(111) under high-pressure conditions at room temperature, but ruled out di-σ-C_2H_4 as the kinetically relevant species.[2,14,16] The same study revealed peaks assigned to surface ethyl species (C_2H_5Pt). By coupling the SFG measurements with on-line GC analysis of the catalyst activity, hydrogenation of π-C_2H_4 to surface C_2H_5Pt and subsequent hydrogenation to ethane was proposed as the main reaction path. π-C_2H_4, di-σ-C_2H_4, and ethyl species were also detected by FT-IR in steady-state hydrogenation experiments over alumina- or MgO-supported Ir clusters,[17] lanthana-supported Rh clusters,[18] or isolated Au centers supported on MgO (π-C_2H_4 and ethyl).[19] On the other hand, the ethylidyne surface species (CH_3CPt_3) familiar from early HREELS and reflection−absorption infrared surface work[9,10,20−23] was determined to play no significant role in the catalytic hydrogenation.[10,24−26] These experimental findings on Pt or Pd surfaces are supported by recent density functional theory (DFT) computational work.[27−30] The calculations predict that the barrier to hydrogenation is substantially lower for π-C_2H_4 than for di-σ-ethylene at the high surface coverage relevant for reaction conditions and that the barrier for ethyl to ethane conversion exceeds that of step 1 by a factor between 2 and 5.

In an attempt to obtain direct evidence for the kinetic relevancy of the ethyl intermediate of C_2H_4 hydrogenation under reaction conditions, we have monitored the catalysis by time-resolved FT-IR spectroscopy using the rapid-scan method. A preliminary study of the catalysis over alumina-supported Pt catalyst at 473 K under continuous $H_2{-}N_2$ flow (1 atm) and pulsed release of C_2H_4 (30 ms duration) revealed two transient intermediates, namely, ethylidyne (2880 and 1339 cm^{-1}) and a species absorbing at 1200 cm^{-1}, assigned to surface ethyl.[31] The rise of both intermediates was too fast to be resolved on

* To whom correspondence should be addressed. E-mail: HMFrei@lbl.gov.

10.1021/jp053773o CCC: $30.25
Published on Web 08/12/2005

the 100 ms time scale. As expected, the decay time of the CH_3-CH_2Pt species (around 100 ms) was faster than that of CH_3-CPt_3 (300 ms). Nevertheless, the lifetimes of the two surface species were surprisingly close. Moreover, the ethane growth was already close to its maximum in the first recorded time slice, suggesting that the ethyl species exhibits dispersive hydrogenation kinetics with the majority of the intermediates reacting at times shorter than 100 ms when running at 473 K.

To establish the kinetic relationship between the decay of the surface ethyl species and the rise of the gas-phase ethane, we have conducted a comprehensive FT-IR study of the temperature (323−473 K) and hydrogen concentration dependence of the temporal behavior of the $C_2H_4 + H_2$ reaction over Pt/Al_2O_3 at 25 ms resolution. Taking advantage of the slower kinetics at the lower temperatures, we show in this paper that the surface ethyl decay coincides with the rate of ethane growth and thus demonstrates directly the kinetic relevancy of the surface ethyl intermediate under reaction conditions.

2. Experimental Section

Time-resolved FT-IR spectra were recorded in the rapid-scan mode on a Bruker model IFS88 spectrometer equipped with a HgCdTe PV detector Kolmar Technologies model KMPV8-1-J2 (8 μm band gap) or a HgCdTe PV detector model KMPV11-1-J2 (12 micron band gap). The mirror velocity was 160 kHz, and the spectral resolution was 4 cm^{-1}. The protocol for obtaining the transient spectra consisted of the recording of 99 interferograms (double-sided/forward−backward) following a C_2H_4 pulse, corresponding to 396 single-sided interferograms. Four spectral time slices of 25 ms duration were extracted from the first and four more from the second forward−backward mirror motion after the ethylene pulse, while the four interferograms of each subsequent forward−backward motion were automatically averaged for *S*/*N* improvement, furnishing spectral time slices at 128 ms resolution. A total of 50 such sets of single-beam spectra generated by 50 ethylene pulses were stored as the result of one experiment. Final time-resolved spectra for a given time delay were obtained by calculating the ratio of each of the 50 corresponding stored single-beam spectra against the single-beam spectrum taken just before the pulse. The 50 ratioed spectra were then averaged to yield the absorbance time slice for a given time delay. The results of 10 such experiments were averaged for further *S*/*N* improvement.

The Al_2O_3-supported, finely divided Pt catalyst (Exxon HFR-100; 5% Pt, calcined at 823 K; BET surface area, 180 $m^2\ g^{-1}$) was prepared in the form of a pressed wafer with an embedded W grid. The latter is made of a 0.49 in. diameter tungsten foil (thickness, 0.002 in.), featuring laser-drilled 0.012 in. holes. The grid, which was held by a Ni jaw similar to a design described by Yates et al.,[32] was electrically heated and the temperature monitored by a thermocouple mounted on the W grid. The catalyst was situated in the center of a home-built 100 cm^3 stainless steel reactor cell equipped with two flange-mounted BaF_2 windows for transmission infrared spectroscopy. The catalyst was transparent in the region of 800−5000 cm^{-1} (reduced sensitivity below 1100 cm^{-1} because of Al−O stretch absorption). The continuous flow of a H_2-N_2 mixture (4.5 L min^{-1}; ratio, 0.053 unless noted otherwise; total pressure, 1 atm) entered the cell through a $^1/_4$ in. tube on one side and exited through an exhaust line on the other. The flow of each gas was regulated by MFC valves (MKS Instruments). Millisecond time resolution was achieved by the synchronization of ethylene pulses of 30 ms duration with the forward motion of the interferometer mirror.[33] The spacing between ethylene pulses was 12.8 s, which assured that all reaction had ceased prior to arrival of a fresh pulse. The pulses were released through a fast value (General Valve Series 99 pulsed valve coupled with an Iota One pulse driver) and contained between 3 and 15 μmol C_2H_4, depending on how far the plug retracted during opening of the valve (controlled by the voltage driving the pulsed valve). The pulses merged with the continuous H_2-N_2 flow 7 cm upstream from the center of the reactor cell. Before each series of experiments, the Pt/Al_2O_3 catalyst was exposed for at least 2 h to a H_2-N_2 flow at 473 K in order to ensure complete reduction of the Pt surface. Ethylene (Matheson, 99.999%), hydrogen (Air Gas, 99.9999%), and nitrogen (Air Gas, 99.9995%) gas were used as received.

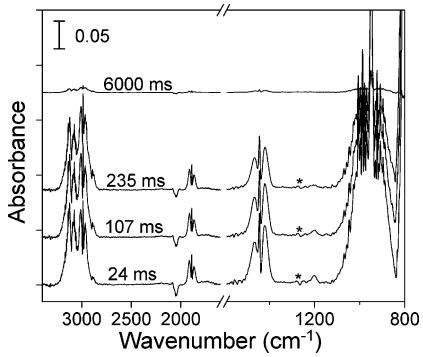

Figure 1. Rapid-scan survey spectra of $C_2H_4 + H_2$ reaction induced by ethylene pulses over Pt/Al_2O_3 at 323 K recorded at 25 ms resolution. Times refer to the time delay between the opening of the pulsed valve and the midpoint of the corresponding interferogram slice. Spectra above 1600 cm^{-1} were recorded with the 8 μm band gap HgCdTe detector; those in the 800−1600 cm^{-1} region, with the 12 μm band gap HgCdTe detector. The derivative-type signal at 1250 cm^{-1} (asterisk) is an effect of the detector. Spectra are displaced vertically for clarity. Small transient bands are best observed in the expanded spectra presented in Figures 3−6.

3. Results

3.1. Reaction at 323 K. Survey spectra of four time slices at 25 ms resolution are shown in Figure 1. The bottom trace is the first spectrum recorded after the C_2H_4 pulse, with its midpoint delayed by 24 ms relative to the opening of the pulsed ethylene valve. Subsequent traces shown are at 107, 235, and 6000 ms. The most prominent bands are the gas-phase absorptions of C_2H_4 at 3000 (ν_9 and ν_{11}), 1890 ($\nu_7 + \nu_8$), 1440 (ν_{12}), and 950 cm^{-1} (ν_7).[34] The ethylene gas-phase bands are the strongest in the first time slice and then decrease, principally due to removal of the reactant from the infrared viewing zone by gas flow.[31] The kinetics of the ethylene decrease is displayed in Figure 2. The depletion observed at 2050 cm^{-1} is attributed to loss of Pt−H absorption.[31,35] The presence of CO, which also absorbs around 2050 cm^{-1}, was ruled out by experiments with D_2.[31]

More interestingly, the spectra reveal additional bands at 2893, 2870, 1339, and 1200 cm^{-1} whose kinetic behavior is very different from that of ethylene. These absorptions, which can be more clearly seen in the expanded spectra of Figures 3−6, were already observed in the 100 ms spectra recorded previously at 473 K and attributed to gas-phase ethane (2893 cm^{-1}, $\nu_8 + \nu_{11}$),[31,36] surface ethylidyne (CH_3CPt_3, 2880 and 1339 cm^{-1}), and surface ethyl species (CH_3CH_2Pt, 2870 and 1200 cm^{-1}).[31] The assignment of the ethyl species is based on the fact that the two bands coincide with known infrared absorptions of surface ethyl intermediates.[31,37,38] On the other hand, the two bands do not agree with the spectra of any other

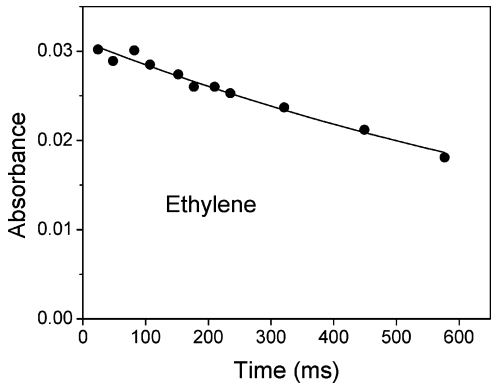

Figure 2. Decrease of ethylene absorption (peak intensity of the 1890 cm^{-1} band) caused by gas flow. A C_2H_4 pulse of 30 ms duration (85 psi back-pressure) was released into a continuous H_2-N_2 flow (4.5 L min^{-1}, 1 atm, $H_2/N_2 = 0.053$) at 323 K.

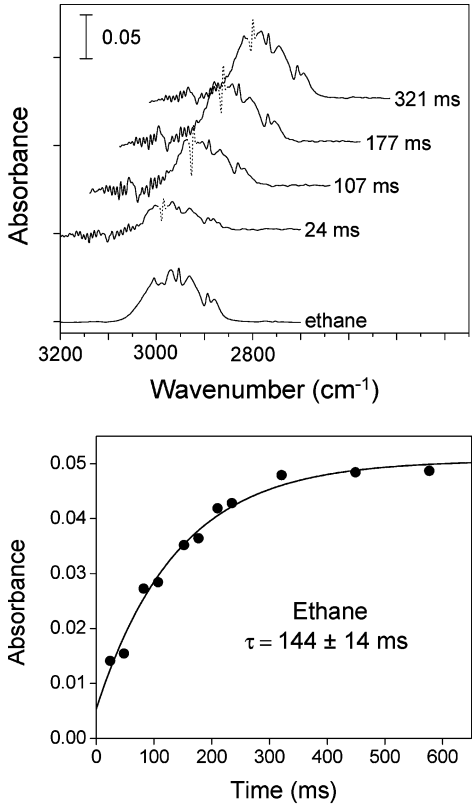

Figure 3. Rapid-scan spectra in the 2700−3200 cm^{-1} region observed following the initiation of $C_2H_4 + H_2$ catalysis at 323 K. The ethylene bands have been subtracted. The bottom trace shows the static spectrum of an authentic ethane sample recorded with the same spectral parameters used for the time-resolved $C_2H_4 + H_2$ runs. The lower panel is the kinetics of ethane growth (peak absorbance at 2893 cm^{-1}). The data points are corrected for absorbance loss due to removal of ethane by gas flow (see text). The solid line represents a single-exponential fit.

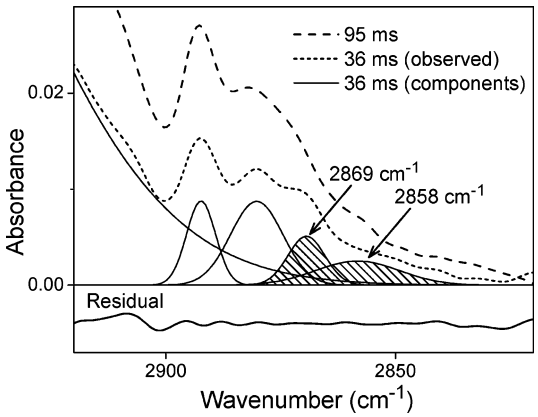

Figure 4. Spectral deconvolution of the 36 ms trace showing the CH stretch absorptions of surface ethyl. The 36 and 95 ms traces represent the averages of the first two and second two time slices after the initiation of catalysis at 323 K. Component bands (Gaussian) and the residual trace resulting from spectral deconvolution (36 ms trace) are displayed (Levenburg−Marquardt method, GRAMS/AI software Version 7.02, Thermo Electron).

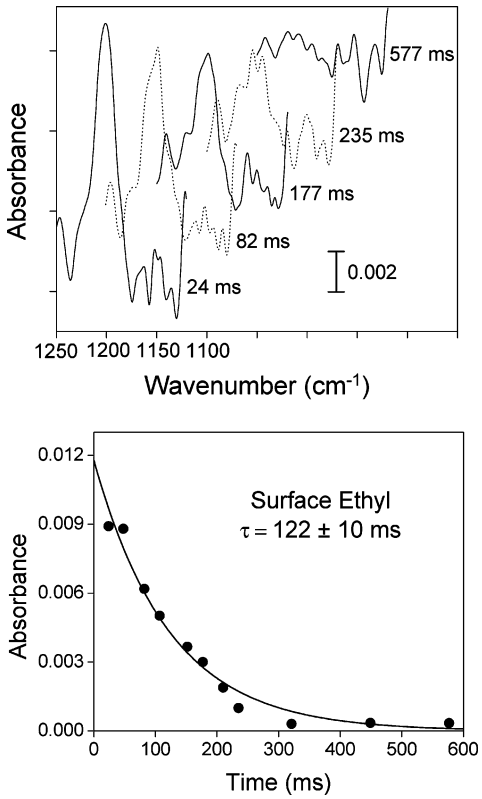

Figure 5. Rapid-scan spectra in the 1120−1250 cm^{-1} region observed following the initiation of $C_2H_4 + H_2$ catalysis at 323 K. The solid curve in the lower panel represents the best fit using a single-exponential function for the peak absorbance of the 1200 cm^{-1} CH_3CH_2Pt band.

surface species whose formation or decay depends on H_2 concentration such as π-C_2H_4 [5−11] or ethylidene.[39] The improved sensitivity, time resolution, and lower reaction temperatures reported here furnish crucial kinetic insights not accessible in our preliminary study. The ethane band at 2893 cm^{-1} grows in during the initial 250 ms period and then starts to decrease. Computer subtraction of C_2H_4 absorption facilitates the kinetic analysis of the ethane band. Precise spectral subtraction is achieved by adjusting the intensity of the C_2H_4 spectrum so that the 1890 cm^{-1} band cancels completely (the region is free of overlap with any other species). The spectra and the absorbance growth fitted by a single-exponential law are shown in Figure 3. Determination of the latter required that each spectral trace was corrected for the loss of product by removal through gas flow, which is evident from the observed decrease of the 2893 cm^{-1} peak at times greater than 250 ms. Since the ethane molecules join the flow of the $C_2H_4-N_2-H_2$ gas mixture upon desorption from the Pt surface, the rate of removal of C_2H_6 from the viewing zone is the same as that of ethylene. Therefore, the C_2H_6 band at time t was normalized by the factor $[C_2H_4]_{24ms}/[C_2H_4]_t$ taken from Figure 2. Comparison with an authentic

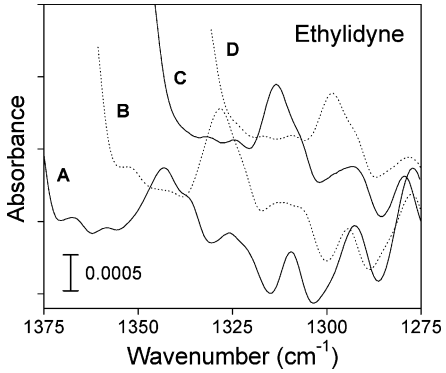

Figure 6. Rapid-scan spectra in the 1275−1375 cm^{-1} region observed following the initiation of $C_2H_4 + H_2$ catalysis at 323 K: (A) $t = 36$ ms; (B) $t = 164$ ms; (C) $t = 321$ ms; (D) $t = 577$ ms.

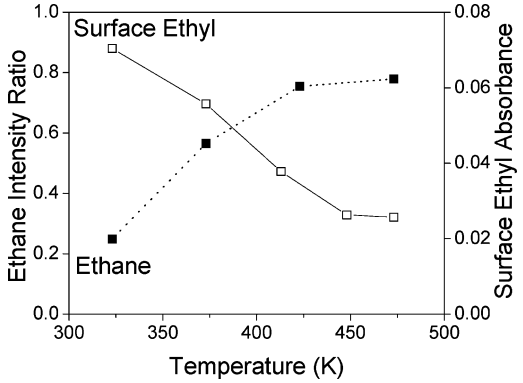

Figure 7. Prompt growth of ethane and of surface ethyl upon C_2H_4 hydrogenation as a function of temperature. The ethane intensity ratio corresponds to the absorbance of the first time slice (24 ms) relative to the asymptotic C_2H_6 growth (2893 cm^{-1}). For surface ethyl, integrated absorbance (1200 cm^{-1}) was used because the bandwidth depends significantly on temperature. Data shown used a flow of 9 L min^{-1} and a H_2/N_2 ratio of 0.027 (ethyl) and 4.5 L min^{-1} ($H_2/N_2 = 0.053$) for ethane.

spectrum of gaseous C_2H_6 recorded with identical spectral parameters (bottom trace of Figure 3) shows that the spectral subtraction reveals the ν_5(CH) mode of ethane at 2954 cm^{-1} in addition to the 2893 cm^{-1} band already observed in the raw spectra.[36] The growth of the two ethane bands is identical within uncertainties, with a 1/*e* rise time of 144 ± 14 ms. The C_2H_6 product also absorbs at 2880 cm^{-1} (P branch of $\nu_8 + \nu_{11}$), but this band is overlapped by surface ethyl absorption in the initial time slices. Ethylidyne is also known to absorb at 2880 cm^{-1}.[11] However, the growth of CH_3CPt_3 is too small at 323 K even on the hundreds of milliseconds time scale for detecting its CH stretch absorption (see below). The surface ethyl species contribution to the spectrum in the ν(CH) region can be seen when comparing the first time slices of Figure 3 ($t = 24$ and 107 ms); the 2880 cm^{-1} peak and the shoulder at 2870 cm^{-1} in the 24 ms spectrum are too strong for sole attribution to ethane, with its gas-phase peak at 2893 cm^{-1}. By contrast, at 107 ms the absorption of CH_3CH_2Pt is overwhelmed completely by the C_2H_6 spectrum. The spectral deconvolution of the average of the first two (36 ms) and second two time slices (95 ms) after initiation of catalysis, Figure 4, reveals peaks at 2869 and 2858 cm^{-1}, in excellent agreement with literature reports of CH_3-CH_2Pt produced by ethylene hydrogenation on Pt.[37]

Figure 5 shows the decay kinetics of the transient 1200 cm^{-1} band assigned to surface ethyl species.[31] We find that the decay time of 122 ± 10 ms obtained by using a single-exponential function is the same within error limits as the rise constant of ethane under identical H_2-N_2 flow conditions. This directly demonstrates that the ethane growth originates from hydrogenation of CH_3CH_2Pt species. Moreover, the rate is within a factor of 2 of the turnover frequency (TOF) over a Pt(111) surface reported for steady-state experiments (323 K, $p_{C_2H_4} = 10$ Torr, $p_{H_2} = 20$ Torr, $p_{N_2} = 80$ Torr).[40] As expected, the rate of surface ethyl decay increases with increasing H_2 flow, reflecting the dependence on H surface coverage. For example, the rates are 4.1 s^{-1} for $H_2/N_2 = 0.027$, and 8.2 s^{-1} for $H_2/N_2 = 0.053$. The higher signal of the ethane absorption in the 2900 cm^{-1} region allowed a more accurate determination of the H_2 concentration dependence of the ethyl to ethane conversion rate. Comparison of the rise times of ethane for $H_2/N_2 = 0.027$, 0.040, and 0.067 gave a reaction order of 1.38 ± 0.07 (323 K), in good agreement with the reaction order determined by classical methods.[40]

Consistent with the known spectator role of ethylidyne, only a very small band is observed at 1339 cm^{-1} immediately after the ethylene pulse (Figure 6). The species grows in with a rise time of 150 ms. This finding confirms the well-known fact that the rate of formation of CH_3CPt_3 is orders of magnitude lower than that of surface ethyl species.[2]

3.2. Temperature Dependence of Surface Ethyl to Ethane Kinetics. At 473 K, the ethane growth was found to reach a maximum in the first time slice after the pulse.[31] The most striking observations upon decrease of the reaction temperature are the gradual appearance of an ethane growth that occurs over tens to hundreds of milliseconds and a decrease of the prompt ethane component in the first time slice. The prompt C_2H_6 growth as a fraction of the asymptotic growth decreases from 0.78 at 473 K to 0.25 at 323 K, as can be seen from Figure 7. Over the same temperature range from 473 to 323 K, the amount of surface ethyl (1200 cm^{-1}) observed in the initial $t = 24$ ms time slice increases 2.7-fold, also shown in Figure 7. By contrast, the temperature dependence of the first-order rate constant of the CH_3CH_2Pt decay is rather weak, decreasing from 6.9 s^{-1} at 473 to 4.1 s^{-1} at 323 K ($H_2/N_2 = 0.027$).

4. Discussion

Our observation by time-resolved FT-IR that the rise of ethane mirrors the decay time of CH_3CH_2Pt establishes the direct kinetic evidence for the surface ethyl as the kinetically relevant intermediate. The finding that surface CH_3CH_2Pt is the rate-limiting species rather than π-C_2H_4 is supported by recent DFT calculations on ethylene hydrogenation over noble metals. The computations consistently predict the activation barrier of π-ethylene to ethyl hydrogenation (step 1) to be substantially lower than the ethyl hydrogenation barrier (step 2). DFT results for C_2H_4 hydrogenation over Pt by Miura et al. give $E_{a,1} = 4$ kcal mol^{-1}, which is much smaller than $E_{a,2} = 27$ kcal mol^{-1}.[29] A similar computational result was obtained by Neurock and Van Santen for C_2H_4 hydrogenation over Pd surfaces, with $E_{a,1} = 9$ kcal mol^{-1} compared to $E_{a,2} = 17$ kcal mol^{-1}.[28] We conclude that surface ethyl to ethane interconversion is the rate-determining step of ethylene hydrogenation under reaction conditions. The fact that the CH_3CH_2Pt growth is complete in a few milliseconds at all temperatures examined (323−473 K) is in agreement with the low activation energy of step 1 predicted by the DFT calculations.

Some prompt growth of ethane is observed at all temperatures. As can be seen from Figure 3, at 323 K the single-exponential fit of the absorbance growth of the 2893 cm^{-1} band gives a prompt C_2H_6 yield, which is about 25% of the asymptotic growth at that temperature. Clearly, part of the surface ethyl species react with substantially faster rates than the majority of

the CH_3CH_2Pt intermediates. The most likely origin of the dispersion of the first-order rate constants is heterogeneity of the surface environment in which the reaction takes place, resulting in varying strength of interaction of the ethyl moiety with the Pt surface. The most weakly interacting intermediates are expected to exhibit the highest hydrogenation rates, the most strongly interacting ones the slowest rates. A recent computational study of C_2H_4 hydrogenation on Pd(111) by Neurock and Van Santen revealed a strong dependence of the CH_3CH_2-Pd bond strength on surface coverage.[28] Specifically, if the adsorbed ethyl and an adsorbed H share a Pd center, the intermediate is destabilized by 7 kcal mol^{-1} due to repulsive interaction, reducing the barrier of hydrogenation in step 2 from 24 to 17 kcal mol^{-1}.[28] A likely origin for the dispersion of the ethyl to ethane hydrogenation rates on Pt/Al_2O_3 catalyst is heterogeneity in the H distribution on the metal surface, resulting in varying degrees of destabilization of the CH_3CH_2Pt species. The fraction of ethyl intermediates undergoing hydrogenation prior to the 24 ms time slice is expected to increase with rising temperature at the expense of the amount of CH_3CH_2Pt formed, in agreement with the results of our measurements (Figure 7). By contrast, the temperature effect on the ethyl decay kinetics in the range of 323−473 K is weak. This is to be expected for a limited measurement window ($t > 24$ ms) in the case of dispersive kinetics: as the temperature is lowered, ethyl species that are hydrogenated at $t < 24$ ms at the higher temperature become observable on the $t > 24$ ms scale, thereby masking the rate decrease of the slower (more stable) ethyl species.

The very large temperature dependence of the intensity ratio of the two surface species CH_3CH_2Pt and CH_3CPt_3 is worth noting. At 473 K, the 1200 cm^{-1} peak of ethyl and the 1339 cm^{-1} band of ethylidyne have the same intensity within a factor of 2,[31] and both species exhibit the maximum buildup in the first spectrum after the pulse. By contrast, at 323 K, only the ethyl growth is complete at $t < 24$ ms, while the ethylidyne band shows a factor of 10 lower intensity in the first time slice and grows in slowly over hundreds of milliseconds. The observed large decrease of the rate of formation of ethylidyne from 473 to 323 K is consistent with the higher barrier for ethylene to ethylidyne dehydrogenation compared to ethylene hydrogenation.[28,41−43] This entails a larger temperature effect on the rate constant that may extend the dehydrogenation from times much shorter than 10 ms to hundreds of milliseconds. The observation of similar amounts of ethyl and ethylidyne in the 473 K experiment merely reflects the fact that most surface CH_3CH_2Pt are already consumed by hydrogenation to C_2H_6 before the 24 ms spectrum is recorded. This results in only a small amount of ethyl species left unreacted after tens of milliseconds.

5. Conclusions

FT-IR monitoring of ethylene hydrogenation over Pt/Al_2O_3 with a time resolution of 25 ms in the temperature range from 323 to 473 K reveals surface ethyl as the rate-limiting reaction intermediate. The hydrogenation of ethylene to CH_3CH_2Pt is instantaneous on the millisecond time scale at all temperatures examined, indicating a substantially lower barrier compared to surface ethyl to ethane conversion. These observations are in agreement with recent DFT calculations reported in the literature. The decay of CH_3CH_2Pt was found to exhibit the same temporal behavior as the rise of C_2H_6, demonstrating directly the kinetic significance of the surface ethyl intermediate for the first time. Dispersive kinetics of the ethyl to ethane hydrogenation manifests the varying strength of interaction of CH_3CH_2 with the Pt surface, which we attribute to heterogeneity of the surface coverage. Computational work on ethylene hydrogenation over a Pd surface by Neurock and Van Santen suggests that the distribution of H on the metal surface is the likely cause of the variation of the ethyl−surface interaction strength.[28] At 323 K, the rise of the ethylidyne spectator species is around 150 ms, consistent with the much higher barrier of ethylene dehydrogenation compared to hydrogenation at high surface coverage. As expected, the rate of CH_3CPt_3 formation increases beyond the millisecond resolution limit of our current experiment when raising the temperature to 473 K. While 25 ms time resolution using the rapid-scan technique coupled with pulsed release of reactants through a mechanical valve proved sufficient for the monitoring of ethyl to ethane hydrogenation, the microsecond and nanosecond resolution of the step-scan FT-IR technique will be required for monitoring the initial ethylene to ethyl hydrogenation step.[33] Furthermore, the limitation of the accessible spectral windows for sensitive monitoring of the surface intermediates due to gas-phase reactant absorption will be addressed by employing the attenuated total reflection method.

Acknowledgment. This work was supported by the Director, Office of Science, Office of Basic Energy Sciences, Division of Chemical, Geological and Biosciences of the U.S Department of Energy, under Contract No. DE-AC03-76SF00098. The authors thank Dr. Joel Ager of LBNL for samples of Pt/Al_2O_3 catalyst and Prof. Gabor Somorjai for insightful discussions.

References and Notes

(1) Zaera, F. *Prog. Surf. Sci.* **2001**, *69*, 1−98.
(2) Somorjai, G. A.; McCrea, K. R. *Adv. Catal.* **2000**, *45*, 385−438.
(3) Srivastava, R. D. *Heterogeneous Catalytic Science*; CRC Press: Boca Raton, FL, 1988.
(4) Horiuti, J.; Polanyi, M. *Trans. Faraday Soc.* **1934**, *30*, 1164−1172.
(5) Cassuto, A.; Mane, M.; Jupille, J. *Surf. Sci.* **1991**, *249*, 8−14.
(6) Demuth, J. E. *Surf. Sci.* **1979**, *84*, 315−328.
(7) Steiniger, H.; Ibach, H.; Lehwald, S. *Surf. Sci.* **1982**, *117*, 685−698.
(8) Zaera, F. *Langmuir* **1996**, *12*, 88−94.
(9) Cremer, P. S.; Stanners, C.; Nremantsverdriet, J.; Shen, Y. R.; Somorjai, G. A. *Surf. Sci.* **1995**, *328*, 111−118.
(10) Mohsin, S. B.; Trenary, M.; Robota, H. J. *J. Phys. Chem.* **1988**, *92*, 5229−5233; *J. Phys. Chem.* **1991**, *95*, 6657−6661.
(11) Sheppard, N.; De La Cruz, C. *Adv. Catal.* **1996**, *41*, 1−112.
(12) Zaera, F.; Chrysostomou, D. *Surf. Sci.* **2000**, *457*, 71−88.
(13) Cremer, P. S.; Su, X.; Somorjai, G. A.; Shen, Y. R. *J. Mol. Catal. A: Chem.* **1998**, *131*, 225−241.
(14) Cremer, P. S.; Su, X.; Shen, Y. R.; Somorjai, G. A. *J. Am. Chem. Soc.* **1996**, *118*, 2942−2949.
(15) Ofner, H.; Zaera, F. *J. Phys. Chem. B* **1997**, *101*, 396−408.
(16) McCrea, K. R.; Somorjai, G. A. *J. Mol. Catal. A: Chem.* **2000**, *163*, 43−53.
(17) Argo, A. M.; Odzak, J. F.; Lai, F. S.; Gates, B. C. *Nature* **2002**, *415*, 623−626.
(18) Bhirud, V.; Goellner, J. F.; Argo, A. M.; Gates, B. C. *J. Phys. Chem. B* **2004**, *108*, 9752−9763.
(19) Guzman, J.; Gates, B. C. *J. Catal.* **2004**, *226*, 111−119.
(20) Kubota, J.; Ichihara, S.; Kondo, J. N.; Domen, K.; Hirose, C. *Langmuir* **1996**, *12*, 1926−1927.
(21) Ohtani, T.; Kubota, J.; Kondo, J. N.; Hirose, C.; Domen, K. *J. Phys. Chem. B* **1999**, *103*, 4562−4565.
(22) Salmeron, M.; Somorjai, G. A. *J. Phys. Chem.* **1982**, *86*, 341−350.
(23) Kesmodel, L. L.; Dubois, L. H.; Somorjai, G. A. *Chem. Phys. Lett.* **1978**, *56*, 267−271.
(24) Davis, S. M.; Zaera, F.; Gordon, B. E.; Somorjai, G. A. *J. Catal.* **1985**, *92*, 240−246.
(25) Beebe, T. P.; Yates, J. T., Jr. *J. Am. Chem. Soc.* **1986**, *108*, 663−671.
(26) Backman, A. L.; Masel, R. I. *J. Vac. Sci. Technol., A* **1991**, *9*, 1789−1792.
(27) Neurock, M.; Pallassana, V.; Van Santen, R. A. *J. Am. Chem. Soc.* **2000**, *122*, 1150−1153.

(28) Neurock, M.; Van Santen, R. A. *J. Phys. Chem. B* **2000**, *104*, 11127−11145.
(29) Miura, T.; Kobayashi, H.; Domen, K. *J. Phys. Chem. B* **2000**, *104*, 6809−6814.
(30) Hirschl, R.; Eichler, A.; Hafner, J. *J. Catal.* **2004**, *226*, 273−282.
(31) Ko, M. K.; Frei, H. *J. Phys. Chem. B* **2004**, *108*, 1805−1808.
(32) Basu, P.; Ballinger, T. H.; Yates, J. T., Jr. *Rev. Sci. Instrum.* **1988**, *59*, 1321−1328.
(33) Yeom, Y. H.; Frei, H. In *In Situ Spectroscopy of Catalysts*; Weckhuysen, B. M., Ed.; American Scientific Publishers: Stevens Ranch, CA, 2004; pp 32−46.
(34) Herzberg, G. *Infrared and Raman Spectra*; Van Nostrand: New York, 1945; pp 325−328.
(35) Pliskin, W. A.; Eischens, R. P. *Z. Phys. Chem. (Munich)* **1960**, *24*, 11−24.
(36) Herzberg, G. *Infrared and Raman Spectra*; Van Nostrand: New York, 1945; pp 342−346.
(37) De La Cruz, C.; Sheppard, N. *J. Mol. Struct.* **1991**, *247*, 25−30.
(38) McGee, K. C.; Driessen, M. D.; Grassian, V. H. *J. Catal.* **1995**, *157*, 730−739.
(39) Deng, R.; Herceg, E.; Trenary, M. *Surf. Sci.* **2004**, *560*, L195−L201.
(40) Zaera, F.; Somorjai, G. A. *J. Am. Chem. Soc.* **1984**, *106*, 2288−2293.
(41) Mohsin, S. B.; Trenary, M.; Robota, H. J. *Chem. Phys. Lett.* **1989**, *154*, 511−515.
(42) Gland, J. L.; Zaera, F.; Fischer, D. A.; Carr, R. G.; Kollin, E. B. *Chem. Phys. Lett.* **1988**, *151*, 227−229.
(43) Lee, A. F.; Wilson, K. *J. Vac. Sci. Technol., A* **2003**, *21*, 563−568.